ISBN: 978-3-95450-232-5 ISSN: 2673-7000 doi:10.18429/JACoW-NAPAC2022-MOZE3

EMITTANCE MEASUREMENTS AND SIMULATIONS FROM AN X-BAND SHORT-PULSE ULTRA-HIGH GRADIENT PHOTOINJECTOR*

G. Chen†, D. Doran, S. Kim, W. Liu, J. Power, C. Whiteford, E. Wisniewski
Argonne National Laboratory, Lemont, IL 60439, USA
C. Jing[1], E. Knight, S. Kuzikov, Euclid Techlabs LLC, Bollingbrook, IL 60440, USA
X. Lu[1], P. Piot[1], W. H. Tan, Northern Illinois University, DeKalb, IL 60115, USA
[1] also at Argonne National Laboratory, Lemont, IL 60439, USA

Abstract

A program is under way at the Argonne Wakefield Accelerator facility, in collaboration with the Euclid Techlabs and Northern Illinois University (NIU), to develop a GeV/m-scale photocathode gun, with the ultimate goal of demonstrating a high-brightness photoinjector beamline. The novel X-band photoemission gun (Xgun) is powered by high-power, short RF pulses, 9-ns (FWHM), which, in turn, are generated by the AWA drive beam. In a previous proof-of-principle experiment, an unprecedented 400 MV/m gradient on the photocathode surface was demonstrated. In the current version of the experiment, we added a linac to the beamline to increase the total energy and gain experience tuning the beamline. In this paper, we report on the very first result of emittance measurement as well as several other beam parameters. This preliminary investigation has identified several factors to be improved on in order to achieve one of the ultimate goals: low emittance.

INTRODUCTION

High brightness photoinjectors are enabling technologies for a host of scientific instruments including future linear colliders, next generation free electron lasers (FELs) [1], compact X-ray sources [2], and ultrafast electron diffraction or microscopy [3, 4]. There are two primary approaches for decreasing the transverse emittance for increasing brightness: lowering the thermal emittance of the photocathode or increasing the gradient of the accelerating field on the cathode surface, Ez. The program underway at the Argonne Wakefield Accelerator (AWA) facility, in collaboration with the Euclid Techlabs and Northern Illinois University (NIU), takes the latter approach by attempting to increase Ez in an RF gun to unprecedented levels. The collaboration is developing an ultra-high gradient X-band gun (Xgun) based on the short RF pulse approach at room temperature, motivated by the fact that the probability of RF breakdown is reduced as the RF pulse length decreases [5].

EXPERIMENTAL SETUP

The experimental layout (Fig. 1) consists of two main sections: the AWA drive beamline and the Xgun beamline.

Table 1: List of Operating Parameters

Parameter	Value	Unit
Drive charge	~270	nC
Laser σ_x	0.189	mm
Laser σ_y	0.234	mm
Laser bunch length (FWHM)	300	fs
Xgun peak E-field	280.0±3	MV/m
Xgun phase[1]	31.8	degree
Bunch charge	45±10	pC
Solenoid B-field	0.202	T
Linac peak field	86.9±2	MV/m

[1] Xgun phase is with respect to the zero phase (see Fig. 2).

The drive linac produces a high-charge drive bunch train (up to 400 nC) which is passed into a power extraction and transfer structure (PETS) [6] to generate a high peak-power short rf pulse (3-ns flat top) at 11.7 GHz. The rf power from the PETS is then transferred through a directional coupler [6] and to the Xgun beamline.

In the section of the Xgun beamline, it consists of a 1.5-cell Xgun (more details on its rf properties can be found in Ref. [7, 8]), a brazeless linac (a structure that was designed for wakefield power extractor [8, 9] but here we reversed its use) for further beam acceleration, a spectrometer dipole for energy measurements, some diagnostics and focusing elements are shown in Fig. 1. Given the extracted rf power from the PETS, a variable power splitter was installed to properly adjust the power ratio between the Xgun and the linac. Additionally, in order to achieve in-phase acceleration in the linac, a phase shifter has been introduced for the linac phase adjustment. In the experiment, the power split ratio between the Xgun and the linac is of 50:50. More details on the power splitter and phase shifter can be found in Ref. [8, 10]. The basic operating parameters are summarized in Table 1.

Xgun Phase Scan

The laser injection phase is controlled by a movable delay stage by adding/subtracting additional laser travel distance, thus change the relative laser arrival time on the cathode. Fig. 2 shows a complete phase scan. The charge was measured by an integrated charge transformer (XICT1 in Fig. 1)

* This work is supported by the U.S. DOE, under award No. DE-SC0018656 to NIU, DOE SBIR grant No. DE-SC0018709 at Euclid Techlabs LLC, and contract No. DE-AC02-06CH11357 with ANL.
† b288079@anl.gov

ISBN: 978-3-95450-232-5 ISSN: 2673-7000 doi:10.18429/JACoW-NAPAC2022-MOZE3

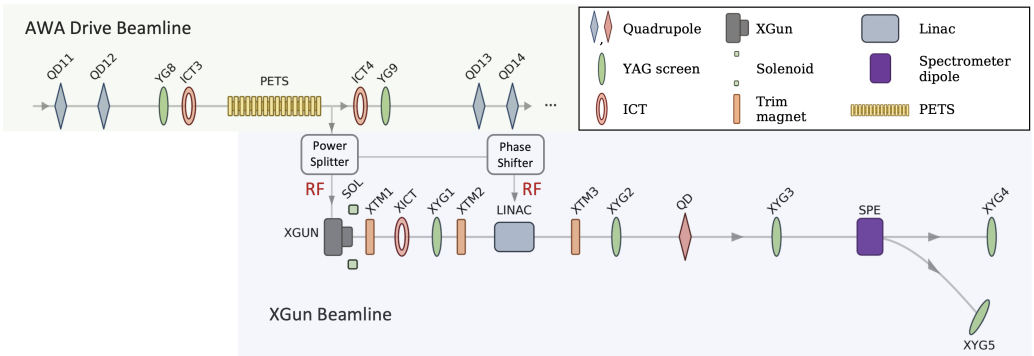

Figure 1: Schematic diagram of the relevant AWA drive beamline and the full Xgun beamline. The element description is shown in the legend.

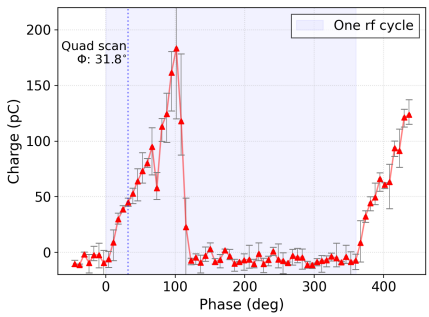

Figure 2: Measured Xgun charge as a function of laser injection phase. The error bars represent the standard deviation of the measured charge caused by machine jitter.

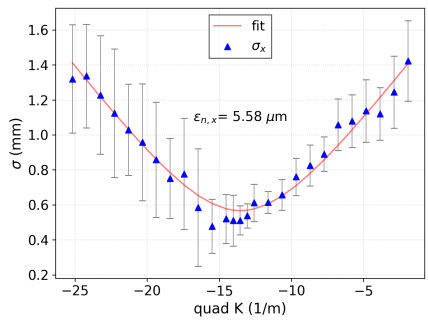

Figure 3: An example of quad scan for horizontal emittance measurement. The solid line is the fitting result. The normalized emittance is calculated and displayed in the plot.

while moving the delay stage. In Fig. 2, the two zero-crossing phases define the range of one rf cycle.

Emittance Measurement with Quad Scan

The launching phase was set to 31.8° referring to the zero phase as shown in Fig. 2. Then the generated electron beam was focused and transferred through the linac. A linac phase scan was performed by measuring the beam energy using the spectrometer dipole while tuning the linac shifter. Then the emittance was measured at the maximum energy gain (~5.9 MeV) of the electron beam.

To measure the emittance, the quadrupole scan method has been applied with the beam profiles captured from a downstream YAG screen (XYG4 in Fig. 1). An example of quad scan for horizontal emittance measurement is shown in Fig. 3. The fitted emittance is evaluated based on the thin-lens approximation. The horizontal and vertical emittance were found to be 5.58 μm and 11.26 μm, respectively. This discrepancy between the x and y emittance is likely related to the geometry asymmetry of the linac design [9, 11], since the side coupler to the linac cell are all on one side along x direction, therefore a large beam fluctuation along x direction occurs. While the vertical emittance was measured, the beam was focused along y direction and defocused along x direction. The instability of the beam position along the x direction makes it challenging to capture the full-beam profile and leads to large uncertainties on σ_y.

ANALYSIS OF THE EMITTANCE RESULTS

The emittance values measured are substantially higher than the Xgun ultimate capability [12], which is to be expected at this early stage of development using a non-optimized beamline. In this section, we present a series of ASTRA beam dynamics simulations in order to understand the results obtained.

The optimized beam parameters toward the lowest emittance will be an important guidance in the experiment. However, owing to practical operating restrictions, for example, non-uniform laser profile, systematic error caused by drive charge stability which can potentially affect the total extracted power from the PETS, it is hard to maintain all parameters same as the optimization. So knowing the sensitivities of different factors to the value of emittance is also of great importance. Based on the used operating parameters in the previous section, a few sets of comparative simulations using ASTRA have been performed to investigate the most possible factors causing the emittance growth and, therefore, help improve the emittance in the future work.

In the present work, possible factors that could contribute to emittance growth include: laser spot size, laser bunch length, Xgun launching phase, solenoid field, linac gradient,

ISBN: 978-3-95450-232-5 ISSN: 2673-7000 doi:10.18429/JACoW-NAPAC2022-MOZE3

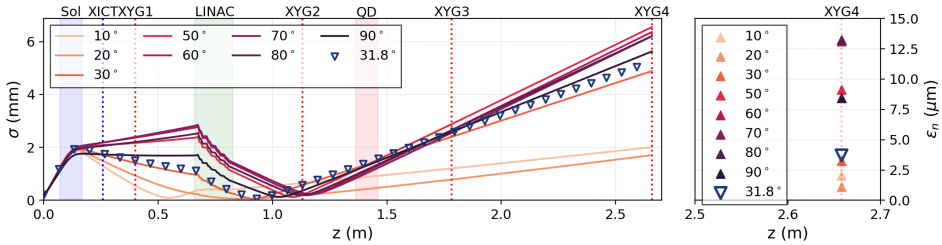

(a) Sim. set#1; effect of different gun launching phases on emittance. Basic simulation parameters can be found in Table 2.

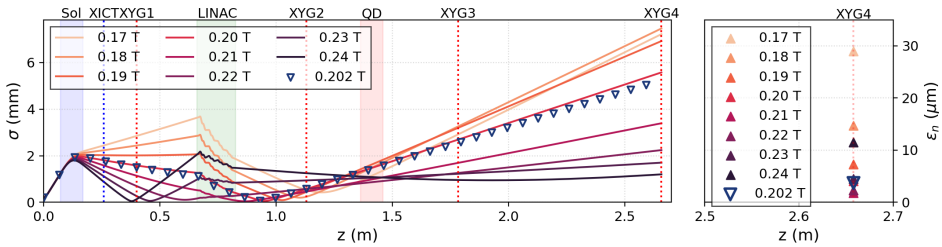

(b) Sim. set#2; effect of different solenoid strengths on emittance. Basic simulation parameters can be found in Table 2.

Figure 4: Two sets of beam dynamics simulations with basic simulation parameters listed in Table 2. The two plots on the left column show the transverse beam size evolution along the longitudinal (z) direction. The two plots on the right column show the simulated emittance at the position of XYG4. The triangles is the simulation using real operating parameters.

Table 2: List of Simulation Parameters

Parameter	Sim. set#1	Sim. set#2
Xgun phase [2]	10° to 90°	31.8°
Solenoid B-field	0.202 T	0.17 T to 0.24 T

[2] Instead of referring the gun phase to the maximum energy gain following ASTRA convention, here the phase is with respect to the zero phase from the simulated Schottky scan [7].

etc. Given the practical operation restrictions and the beamline element dimension limitations at AWA, the laser spot size and the laser bunch length have a relatively small tunable range, and were found to be less sensitive to the simulated emittance comparing to other factors. Then, by scanning the control parameters of the Xgun launching phase and the solenoid field, their effect on emittance have been studied individually. The basic simulation parameters are listed in Table 2.

To validate the reliability of the simulation, the emittance was simulated by using all real operating parameters as shown in Table 1. The simulated emittance at the position of XYG4 (same position for the quad scan) was found to be 3.7 μm (Fig. 4), in reasonable agreement with the measured horizontal emittance of 5.58 μm, since the uncertainties on the machine jitter were not considered in the simulation. It has been found that the emittance can still be greatly improved to the level of 1 μm by carefully adjusting the Xgun phase and the solenoid strength. Additionally, the final emittance is extremely sensitive to the solenoid strength, as expected from the emittance-compensation process [13]. Based on the simulation, to have the lowest emittance, the beam size before the linac needs to be minimized.

FUTURE STUDY

From the measured emittance, a large emittance growth on the vertical direction was noticed which is likely due to the geometry asymmetry of the linac, since the side coupler to the linac cell are all on one side. Thus, a new linac design is proposed and under construction. Additionally, based on the beam dynamics simulations, the emittance was found to be particularly sensitive to the solenoid strength, which directly correlates to the transverse beam size at the entrance of the linac. In order to acquire accurate transverse beam profiles right before the linac, an additional YAG screen is planning to be installed. Characterizing the Xgun at higher gradient toward the optimized operating parameters [12] will be the next step.

CONCLUSION

We report on the very first result of emittance measurement of the Xgun as well as several other beam parameters. The x and y emittance were found to be 5.58 μm and 11.26 μm, respectively, which are more than one order of magnitude higher than the emittance under the optimal beam line parameter set. Plausible reasons have been identified. Measures will be taken to achieve the best beam conditions for future experiments.

ISBN: 978-3-95450-232-5 ISSN: 2673-7000 doi:10.18429/JACoW-NAPAC2022-MOZE3

REFERENCES

[1] P. Emma, R. Akre, J. Arthur, R. Bionta, C. Bostedt, J. Bozek, A. Brachmann, P. Bucksbaum, R. Coffee, F.-J. Decker, *et al.,* "First lasing and operation of an ångstrom-wavelength free-electron laser", *Nature Photon* vol. 4, pp. 641–647, 2010. doi:10.1038/nphoton.2010.176

[2] W. S. Graves, J. Bessuille, P. Brown, S. Carbajo, V. Dolgashev, K.-H. Hong, E. Ihloff, B. Khaykovich, H. Lin, K. Murari, E. A. Nanni, G. Resta, S. Tantawi, L. E. Zapata, F. X. Kärtner, and D. E. Moncton, "Compact x-ray source based on burst-mode inverse Compton scattering at 100 kHz", *Phys. Rev. ST Accel. Beams*, vol. 17, p. 120701, 2014. https://doi.org/10.1103/PhysRevSTAB.17.120701

[3] F. Qi, Z. Ma, L. Zhao, Y. Cheng, W. Jiang, C. Lu, T. Jiang, D. Qian, Z. Wang, W. Zhang, P. Zhu, X. Zou, W. Wan, D. Xiang, and J. Zhang, "Breaking 50 Femtosecond Resolution Barrier in MeV Ultrafast Electron Diffraction with a Double Bend Achromat Compressor", *Phys. Rev. Lett.,* vol. 124, p. 134803, 2020. doi:10.1103/PhysRevLett.124.134803

[4] R. Li and P. Musumeci, "Single-Shot MeV Transmission Electron Microscopy with Picosecond Temporal Resolution", *Phys. Rev. Applied,* vol. 2, p. 024003, 2014. doi:10.1103/PhysRevApplied.2.024003

[5] V. Dolgashev, S. Tantawi, Y. Higashi, and B. Spataro, "Geometric dependence of radio-frequency breakdown in normal conducting accelerating structures", *Appl. Phys. Lett.,* vol. 97, no. 17, p. 171501, Oct. 2010. doi:10.1063/1.3505339

[6] J. H. Shao *et al.*, "Generation of High Power Short Rf Pulses using an X-Band Metallic Power Extractor Driven by High Charge Multi-Bunch Train", in *Proc. IPAC'19*, Melbourne, Australia, May 2019, pp. 734–737. doi:10.18429/JACoW-IPAC2019-MOPRB069

[7] W. H. Tan, S. Antipov, D. S. Doran, G. Ha, C. Jing, E. Knight, S. Kuzikov, W. Liu, X. Lu, P. Piot, J. G. Power, J. Shao, C. Whiteford, and E. E. Wisniewski, "Demonstration of sub-GV/m Accelerating Field in a Photoemission Electron Gun Powered by Nanosecond X-Band Radiofrequency Pulses," 2022. doi:10.48550/arxiv.2203.11598

[8] S. V. Kuzikov *et al.*, "An X-Band Ultra-High Gradient Photoinjector", in *Proc. IPAC'21*, Campinas, Brazil, May 2021, pp. 2986–2989. doi:10.18429/JACoW-IPAC2021-WEPAB163

[9] S. P. Antipov, P. V. Avrakhov, V. A. Dolgashev, D. S. Doran, C.-J. Jing, S. V. Kuzikov, *et al.*, "High Power Tests of Brazeless Accelerating Structures", in *Proc. IPAC'21*, Campinas, SP, Brazil, May 2021, pp. 532–534. doi:10.18429/JACoW-IPAC2021-MOPAB152

[10] S. V. Kuzikov, G. Chen, C.-J. Jing, E. W. Knight, P. Piot, W. H. Tan, *et al.*, "Toward Emittance Measurements at 11.7 GHz Short-Pulse High-Gradient RF Gun", in *Proc. IPAC'22*, Bangkok, Thailand, Jun 2022, pp. 649–651. doi:10.18429/JACoW-IPAC2022-MOPOMS013

[11] S. V. Kuzikov, S. P. Antipov, E. Gomez, and A. A. Vikharev, "High-Gradient Short Pulse Accelerating Structures", in *Proc. NAPAC'19*, Lansing, MI, USA, Sep. 2019, pp. 500–502. doi:10.18429/JACoW-NAPAC2019-TUPLH07

[12] W. H. Tan, G. Chen, G. Ha, C.-J. Jing, S. V. Kuzikov, and P. Piot, "Beam Dynamics Simulations in a High-Gradient X-Band Photoinjector", in *Proc. IPAC'21*, Campinas, Brazil, May 2021, pp. 4013–4016. doi:10.18429/JACoW-IPAC2021-THPAB129

[13] L. Serafini and J. B. Rosenzweig, "Envelope analysis of intense relativistic quasilaminar beams in rf photoinjectors: mA theory of emittance compensation", *Phys. Rev. E*, vol. 55, p. 7565, Jun. 1997. doi:10.1103/PhysRevE.55.7565